Theory of high-harmonic generation by low-frequency laser fields

M. Lewenstein,[1,*] Ph. Balcou,[2] M. Yu. Ivanov,[3,†] Anne L'Huillier,[2,4] and P. B. Corkum[3]
[1]*Joint Institute for Laboratory Astrophysics, University of Colorado, Boulder, Colorado 80309-0440*
[2]*Service des Photons, Atomes et Molécules, Centre d'Etudes de Saclay, 91191 Gif sur Yvette, France*
[3]*National Research Council of Canada, M-23A, Ottawa, Ontario, Canada K1A OR6*
[4]*Lawrence Livermore National Laboratory, L-443, P.O. Box 5508, Livermore, California 94550*
(Received 19 August 1993)

We present a simple, analytic, and fully quantum theory of high-harmonic generation by low-frequency laser fields. The theory recovers the classical interpretation of Kulander *et al.* in [*Proceedings of the SILAP III Workshop*, edited by B. Piraux (Plenum, New York, 1993)] and Corkum [Phys. Rev. Lett. **71**, 1994 (1993)] and clearly explains why the single-atom harmonic-generation spectra fall off at an energy approximately equal to the ionization energy plus about three times the oscillation energy of a free electron in the field. The theory is valid for arbitrary atomic potentials and can be generalized to describe laser fields of arbitrary ellipticity and spectrum. We discuss the role of atomic dipole matrix elements, electron rescattering processes, and of depletion of the ground state. We present the exact quantum-mechanical formula for the harmonic cutoff that differs from the phenomenological law $I_p + 3.17U_p$ where I_p is the atomic ionization potential and U_p is the ponderomotive energy, due to the account for quantum tunneling and diffusion effects.

PACS number(s): 42.65.Ky, 32.80.Rm

I. INTRODUCTION

In recent years, high-order harmonic generation (HG) has become one of the major topics of multiphoton physics [1]. When an intense short-pulse laser interacts with an atomic gas, the atoms respond in a nonlinear way and emit coherent radiation at frequencies that are multiples of the laser frequency. In order to produce high-order harmonics and consequently to generate high-energy photons, one can use either high-frequency excimer (e.g., KrF) lasers ([2,3]) or low-frequency lasers (Nd:glass, Ti:sapphire) such that the laser frequency ω is much smaller than the ionization potential. In the latter case the harmonic spectrum has a very characteristic and universal shape: it falls off for the first few harmonics, then exhibits a *plateau* where all the harmonics have the same strength, and ends up with a sharp *cutoff*. Several groups (see, for example, [4,5] and references therein) have performed experiments in which they observed generation of harmonics of the 100th and higher order, extending as far as 150 eV.

One of the most interesting questions regarding these harmonic-generation spectra concerns the nature and location of the cutoff. Obviously, this question is of great importance from the point of view of possible applications. The cutoff location sets the ultimate limit for the highest frequency that can be efficiently generated. Numerical calculations of Krause *et al.* [6] have shown that the maximum energy at the end of the plateau is well approximated by the simple and universal formula $I_p + 3U_p$, where I_p is the atomic ionization potential, while $U_p = E^2/4\omega^2$ is the ponderomotive energy in the laser field of strength E and frequency ω. U_p is the mean kinetic energy aquired by a free electron in the oscillating laser field of the strength E. The cutoff in the harmonic spectrum occurs for harmonics of order higher than

$$N_{\max} \simeq (I_p + 3U_p)/\omega. \quad (1)$$

The overall maximal photon energy (in units of ω) that can be achieved is then approximately given by the value of this expression at the saturation intensity $I_{\rm sat}$ at which the atom ionizes. Note, however, that Eq. (1) determines the location of the cutoff in a single-atom spectrum. It can be modified when collective effects (phase matching) become relevant [7].

A very important insight into the physical understanding of this cutoff law formula has recently been given by Kulander *et al.* [8] and by Corkum [9], using a semiclassical approach. In this model, electrons first tunnel through the barrier formed by the atomic potential and the laser field [10,11] and appear in the continuum with zero velocity. Their subsequent motion in the field is treated classically. Only those electrons that return to the nucleus can emit harmonics by recombining to the ground state. Classical simulations [8,9] show that the maximum kinetic energy acquired by the free electrons from the field when they return to the nucleus is $3.2U_p$. Thus the maximal energy of emitted photons is $I_p + 3.2U_p$, close to the prediction of [6]. The semiclassical approach is based on three basic assumptions. The dominant contribution to HG comes from electrons that (i) return to the nucleus, (ii) appear in the continuum with zero velocity, and (iii) finally, have an appropri-

*Permanent address: Centrum Fizyki Teoretycznej PAN, Al. Lotników 32/46, 02–668 Warsaw, Poland.
†Permanent address: General Physics Institute, Vavilov Str. 38, Moscow 117942, Russia.

ate kinetic energy to produce a given harmonic at the time of return. This classical interpretation shows that in order to control harmonic-generation processes, one should try to control the motion of free electrons in the laser field. Shaping appropriately electron trajectories might allow for various fascinating applications, including, for example, the generation of subfemtosecond high-frequency pulses [12].

In a recent paper [7], we have discussed the harmonic-generation cutoff in a low-frequency high-intensity regime, presenting experimental data and calculations involving the response of a single-atom and of the macroscopic medium. Systematic measurements of the harmonic generation yields in neon have been performed using a short-pulse low-frequency laser. The experimental cutoff energy was found to be approximately $I_p + 2U_p$, therefore lower than that predicted in single-atom theories [9,6,13]. A simple, analytic, and fully quantum-mechanical theory of harmonic generation valid in the tunneling limit has been formulated. It agrees well with the predictions of other single-atom theories and in particular with the cutoff law. It recovers the semiclassical interpretation of harmonic generation in this low-frequency regime. The difference between the prediction for the single-atom cutoff and the experimental results have been explained by accounting for the influence of propagation effects [14] in a tight focusing geometry [7]. A good agreement between theory and experiment has been obtained.

In the present paper, we give a full account of the theoretical part of Ref. [7] which deals with the response of a single atom. Propagation effects will be discussed in a future paper. We give a detailed formulation of the theory with, in particular, a discussion of its range of validity. We study different potentials and we investigate the influence of the various relevant parameters. One could argue that the fully quantum and exact theory of HG has been already formulated in terms of the solution of the time-dependent Schrödinger equation (TDSE) [6,15–18] or, equivalently, in terms of the solution of the time-independent Floquet equations [19]. On the other hand, the simple quasiclassical model of Refs. [8,9] allows for a physical interpretation of the results of Ref. [6]. Therefore, at first sight, there is no need for any approximate theory that would link the two mentioned approaches. However, the TDSE method requires a lot of computer time. In particular, although it works well for linearly polarized laser fields, it cannot be easily extended, for the time being, to elliptically polarized fields or nonmonochromatic fields with a time-dependent polarization. In contrast, the present theory can easily describe the interaction with laser light of arbitrary polarization and frequency content, allowing one to study strong-field coherent control of high-harmonic emission, for example in the field of two lasers with related frequencies. On the other hand, the semiclassical approach used in Refs. [8,9] mixes classical and quantum arguments (first quantum tunneling, then classical motion, then quantum recombination). It does not account for many important quantum effects, such as quantum diffusion of wave packets, quantum interferences, etc. The motivation of the present work was to find an intermediate approximate solution to the problem of harmonic generation valid in a low-frequency high-intensity regime that would provide a link between the methods of Refs. [6] and [8,9], on one hand, and would allow one to study the effects of multicolor or elliptically polarized light on harmonic generation, on the other hand.

Recently, several authors [20–22] have emphasized the importance of bound states in harmonic generation on the formation of the plateau (see also [23,24]). Other cutoff laws, different from Eq. (1), e.g., involving Rabi frequencies, have been derived [21,22]. The present theory applies to a regime of parameters where bound states should be relatively unimportant: it is valid in a low-frequency, high intensity limit ($U_p \geq I_p$), and for high harmonics, with energy higher than, say, the ionization energy. It is well adapted to a discussion of the cutoff location, but it obviously cannot describe well those low-order harmonics below or just above the ionization limit. On the other hand, it includes important quantum-mechanical effects such as quantum diffusion, quantum interferences, depletion of the ground state which are not included in the classical approaches [8,9,25] and it allows us to get a better physical understanding of harmonic generation in the tunneling limit.

The plan of the paper is the following. Section II contains a general presentation of our theory and a discussion of its quasiclassical interpretation. We present general expressions for harmonic spectra and harmonic strengths. Section III is divided into several subsections in which we describe applications of our theory to various model potentials. In particular, we study the case of a transition from a $1s$ state to a continuum for a Gaussian model and also for hydrogenlike atoms. We address the question of electron rescattering, i.e., the process in which the electron returning to the nucleus is scattered away from it instead of being recombined. In Sec. IV, we reexamine our theory using the saddle-point technique. The most important result of this section is the derivation of the quantum-mechanical cutoff law. We find that it actually differs from the phenomenological expression $I_p+3.17U_p$ and has a form $3.17U_p+I_pF(I_p/U_p)$ where the factor $F(I_p/U_p)$ is equal to 1.3 for $I_p \ll U_p$ and decreases slowly towards 1 as I_p grows. In Sec. V, we discuss the effects of saturation and depletion of the atomic ground state. Finally, Sec. VI contains the conclusions, whereas the Appendixes A and B are devoted to some more technically involved derivations of the formulas used in the main body of the paper.

II. THEORY OF HARMONIC GENERATION

The theoretical problem that we attempt to solve is the same as in the case of the TDSE method. We consider an atom (or an ion) in a single-electron approximation under the influence of the laser field $E\cos(t)$ of linear polarization in the x direction (we use atomic units, but express all energies in terms of the photon energy). In the length gauge, the Schrödinger equation takes the form

$$i|\Psi(\mathbf{x},t)\rangle = \left[-\frac{1}{2}\nabla^2 + V(\mathbf{x}) - E\cos(t)x\right]|\Psi(\mathbf{x},t)\rangle. \quad (2)$$

Initially, the system is in the ground state, denoted as $|0\rangle$, which in general has a spherical symmetry.

We consider the case when $I_p \gg 1$ (typically $I_p \simeq 5-20$ laser photons) and when U_p is comparable or larger than I_p. We start our discussion by considering the case when ionization is weak, so U_p should be large, but still below the saturation level, $U_{\rm sat}$, when all atoms ionize during the interaction time. In this regime of parameters, the tunneling theory [10,11] becomes valid [26]. The intensities are large enough (10^{14}–10^{15} W/cm^2) so that intermediate resonances, including dynamically induced ones (see, for instance, [27]), play no role. The electron leaves the atoms typically when the field reaches its peak value. The effects of the force due to the potential, $-\nabla V(\mathbf{x})$, is then negligible. The electron undergoes transitions to continuum states which we label by the kinetic momentum of the outgoing electron $|\mathbf{v}\rangle$. As it is accelerated in the field, it immediately acquires a high velocity, so that the role of $V(\mathbf{x})$ is even less pronounced. That is particularly true if the electron returns to the nucleus with a large kinetic energy of the order of $3U_p$. At the turning points, the electron velocity might be quite small but these points are located typically very far from the nucleus.

The above considerations suggest that the following assumptions should be valid in the regime of parameters that we consider.

(a) The contribution to the evolution of the system of all bound states except the ground state $|0\rangle$ can be neglected.

(b) The depletion of the ground state can be neglected ($U_p < U_{\rm sat}$).

(c) In the continuum, the electron can be treated as a free particle moving in the electric field with no effect of $V(\mathbf{x})$.

Assumption (b) can be used only for intensities smaller then saturation intensity. Otherwise, the depletion of the ground state has to be taken into account, as discussed in Sec. V. Assumption (c) is non-questionable for short-range potentials, but is also valid for hydrogenlike atoms, provided U_p is large enough. It is important, however, to be aware of what is the regime of validity of the assumptions (a) and (c). Generally speaking, they hold when there are no intermediate resonances and when the Keldysh parameter $\gamma = \sqrt{I_p/2U_p}$ is smaller then one, i.e., in the tunneling or over-the-barrier ionization regimes. The latter condition requires $I_p \leq 2U_p$ and implies that (i) when the electron appears in the continuum it is under the influence of a very strong laser field, and (ii) when it comes back to the nucleus it has a large kinetic energy, so that the atomic potential force can be neglected. Obviously, the latter implication concerns only highly energetic electrons, responsible for the production of harmonics of order $2M+1 \geq I_p$.

There are several theoretical approaches that incorporate assumption (c) in solving Eq. (2). Ammosov *et al.* study the "classical" dynamics of the electron with time in the complex plane in order to describe tunneling ionization. Keldysh used a version of the $\hat{S}$-matrix theory with final states described by Volkov wave functions ([10], see also [28]), i.e., solutions of the Schrödinger equation describing the motion of a free electron in the laser field. An alternative approach based on the time-reversed $\hat{S}$-matrix theory and called strong-field approximation has been proposed by Reiss [29].

We prefer to follow Ref. [30], since this approach is more closely related to standard methods of quantum optics, in the sense that it neglects, or treats as a perturbation, part of the interaction Hamiltonian. In particular, we put emphasis on the role of a singular part of continuum-continuum (C-C) dipole matrix elements. The most singular part of these matrix elements, $\langle\mathbf{v}|\mathbf{x}|\mathbf{v}'\rangle$, is $i\nabla_{\mathbf{v}}\delta(\mathbf{v}-\mathbf{v}')$. The other parts of the C-C dipole matrix element are either less singular or regular, and we shall neglect them in the following. Although such a procedure might be incorrect in the context of Above-Threshold Ionization [31], it should be reasonable for HG, since C-C transitions between the states of different energies do not contribute to it [32]. The singular part of the C-C dipole matrix elements $i\nabla_{\mathbf{v}}\delta(\mathbf{v}-\mathbf{v}')$ is treated by us exactly. It describes the motion of the free electron in the laser field. It is worth stressing that the part of C-C matrix elements that we neglect may be treated as a perturbation and one can systematically account for corrections to the solution of the Schrödinger equation coming from this perturbation (see Ref. [30]). We should also mention that our method is very similar to the one used in Ref. [13] for the case of a zero range potential. Our approach is, however, more general and can be applied to any potential.

After making the assumptions (a)–(c), the time-dependent wave functions can be expanded as

$$|\Psi(t)\rangle = e^{iI_p t}\left(a(t)|0\rangle + \int d^3\mathbf{v}\, b(\mathbf{v},t)|\mathbf{v}\rangle\right), \quad (3)$$

where $a(t) \simeq 1$ is the ground-state amplitude, and $b(\mathbf{v},t)$ are the amplitudes of the corresponding continuum states. We have factored out here free oscillations of the ground-state amplitude with the bare frequency I_p. The Schrödinger equation for $b(\mathbf{v},t)$ reads as

$$\dot{b}(\mathbf{v},t) = -i\left(\frac{\mathbf{v}^2}{2} + I_p\right)b(\mathbf{v},t) - E\cos(t)\,\frac{\partial b(\mathbf{v},t)}{\partial v_x} + iE\cos(t)\,d_x(\mathbf{v}). \quad (4)$$

Here $\mathbf{d}(\mathbf{v}) = \langle\mathbf{v}|\mathbf{x}|0\rangle$ denotes the atomic dipole matrix element for the bound-free transition and $d_x(\mathbf{v})$ is the component parallel to the polarization axis. In writing Eq. (4) we have neglected the depletion of the ground state, setting $a(t)=1$ on the right-hand side. The whole information about the atom is thus reduced to the form of $\mathbf{d}(\mathbf{v})$, and its complex conjugate $\mathbf{d}^*(\mathbf{v})$.

The Schrödinger Eq. (4) can be solved exactly and $b(\mathbf{v},t)$ can be written in the closed form,

$$b(\mathbf{v},t) = i\int_0^t dt' E\cos(t')d_x(\mathbf{v}+\mathbf{A}(t)-\mathbf{A}(t')) \times\exp\left\{-i\int_{t'}^t dt''\left[(\mathbf{v}+\mathbf{A}(t)-\mathbf{A}(t''))^2/2 + I_p\right]\right\}, \quad (5)$$

where $\mathbf{A}(t) = (-E\sin(t), 0, 0)$ is the vector potential of the laser field.

In order to calculate the x component of the time-dependent dipole moment, we have to evaluate $x(t) = \langle\Psi(t)|x|\Psi(t)\rangle$. Using Eqs. (3) and (5) we obtain

$$x(t) = \int d^3\mathbf{v} d_x^*(\mathbf{v}) b(\mathbf{v}, t) + \text{c.c.} \tag{6}$$

In writing the above formula, we have neglected the contribution from the C-C part [32], i.e., we have considered only the transitions back to the ground state. Introducing a new variable which is a canonical momentum

$$\mathbf{p} = \mathbf{v} + \mathbf{A}(t) \tag{7}$$

we get the final expression

$$x(t) = i\int_0^t dt' \int d^3\mathbf{p}\, E\cos(t') d_x(\mathbf{p} - \mathbf{A}(t')) \times d_x^*(\mathbf{p} - \mathbf{A}(t)) \exp\left[-iS(\mathbf{p}, t, t')\right] + \text{c.c.}, \tag{8}$$

where

$$S(\mathbf{p}, t, t') = \int_{t'}^t dt'' \left(\frac{[\mathbf{p} - \mathbf{A}(t'')]^2}{2} + I_p\right). \tag{9}$$

Equation (8) has a nice physical interpretation [33] as a sum of probability amplitudes corresponding to the following processes: The first term in the integral, $E\cos(t')d_x(\mathbf{p} - \mathbf{A}(t'))$, is the probability amplitude for an electron to make the transition to the continuum at time t' with the canonical momentum $\mathbf{p}$. The electronic wave function is then propagated until the time t and acquires a phase factor equal to $\exp[-iS(\mathbf{p}, t, t')]$, where $S(\mathbf{p}, t, t')$ is the quasiclassical action. The effects of the atomic potential are assumed to be small between t' and t, so that $S(\mathbf{p}, t, t')$ actually describes the motion of an electron freely moving in the laser field with a constant momentum $\mathbf{p}$. Note, however, that $S(\mathbf{p}, t, t')$ does incorporate some effects of the binding potential through its dependence on I_p. The electron recombines at time t with an amplitude equal to $d_x^*(\mathbf{p} - \mathbf{A}(t))$, which gives the last factor entering Eq. (8).

Strictly speaking, Eq. (7) defines the canonical momentum at time t, which does not have to be the same as $\mathbf{p}$ at t'. Note, however, that between t' and t, $\mathbf{p}$ is a conserved quantity, due to neglection of the effects of $V(\mathbf{x})$. For this reason, our interpretation is correct, since we can identify $\mathbf{p}$ equally well as a canonical momentum at t' or t. It is worth stressing that Eq. (8) allows also for an alternative interpretation in which the electron appears in the continuum at time t with the kinetic momentum $\mathbf{p} - \mathbf{A}(t)$, is then propagated back until t', and recombines back to the ground state $|0\rangle$ with the amplitude $E\cos(t')d_x(\mathbf{p} - \mathbf{A}(t'))$. This interpretation is not as intuitive as the previous one, but, owing to the invariance of the problem with respect to time reversal, is equally correct. This is an example of a situation in which approximate versions of the ordinary $\hat{S}$ matrix and time-reversed $\hat{S}$ matrix approaches give the same results (compare with Ref. [29]). Another way of looking at Eq. (8) is to interpret it as a Landau-Dyhne formula for transition probabilities applied to the evaluation of the observable x [33]. Finally, note that Eq. (8) is evidently gauge invariant.

The expression (8) can be easily generalized to the case of laser fields $\mathbf{E}(t)$ of arbitrary polarization and temporal shape. If we want to evaluate the component of the time-dependent dipole moment along the direction $\mathbf{n}$, where $\mathbf{n}$ is an unit vector, the result is

$$x_{\mathbf{n}}(t) = i\int_0^t dt' \int d^3\mathbf{p}\, \mathbf{n}\cdot\mathbf{d}^*(\mathbf{p} - \mathbf{A}(t)) \times \mathbf{E}(t')\cdot\mathbf{d}(\mathbf{p} - \mathbf{A}(t')) \exp\left[-iS(\mathbf{p}, t, t')\right] + \text{c.c.}, \tag{10}$$

In the present work, we shall restrict ourselves to the simple case of the linearly polarized monochromatic field, with the time-dependent dipole moment given by Eq. (8). The dipole matrix elements that enter Eq. (8) change typically on a scale of the order of $p^2 \simeq I_p$. On the other hand, the quasiclassical action (9) changes on a characteristic scale $p^2 \simeq 1/(t - t')$, due to quantum diffusion effects. For $t - t'$ of the order of one period of the laser field the quasiclassical action varies thus much faster than the other factors entering Eq. (8). Therefore, the major contribution to the integral over $\mathbf{p}$ in Eq. (8) comes from the stationary points of the classical action,

$$\nabla_{\mathbf{p}} S(\mathbf{p}, t, t') = \mathbf{0}. \tag{11}$$

On the other hand, $\nabla_{\mathbf{p}} S(\mathbf{p}, t, t')$ is nothing else but the difference between the position of the free electron at time t and time t',

$$\nabla_{\mathbf{p}} S(\mathbf{p}, t, t') = \mathbf{x}(t) - \mathbf{x}(t'). \tag{12}$$

Therefore we conclude that the stationary points of the classical action correspond to those momenta $\mathbf{p}$ for which the electron born at time t' returns to the the same position at time t. It is also evident that $\mathbf{x}(t)$ must be close to the origin, because it is the only position where the transitions to the ground state (and from the ground state) can possibly occur. Mathematically, this statement follows from the fact that the Fourier transforms of $d_x(\mathbf{p} - \mathbf{A}(t'))$ and $d_x^*(\mathbf{p} - \mathbf{A}(t))$ are localized around the nucleus on a scale comparable to a_0, where a_0 is the Bohr radius.

The physical meaning of the mathematical result expressed by Eq. (12) is clear: the dominant contribution to the harmonic emission comes from the electrons which tunnel away from the nucleus but then reencounter it while oscillating in the laser field. Thus, our quantum theory justifies one of the basic assumptions of the semiclassical model of Refs. [8,9].

According to the above discussion, the integral over $\mathbf{p}$ might be performed using a saddle-point method. The result is

$$x(t) = i\int_0^\infty d\tau \left(\frac{\pi}{\epsilon + i\tau/2}\right)^{3/2} d_x^*(p_{st}(t, \tau) - A_x(t)) \times d_x(p_{st}(t, \tau) - A_x(t - \tau)) E\cos(t - \tau) \times \exp[-iS_{\text{st}}(t, \tau)] + \text{c.c.} \tag{13}$$

In writing Eq. (13), we have introduced a new variable (the return time) $\tau = t - t'$ and extended integration over it to ∞. The stationary value of the xth component of the momentum, $p_{\rm st}(t,\tau)$, allows the electron trajectory starting near the origin at $t-\tau$ to return to the same position at t. It is equal to

$$p_{\rm st}(t,\tau) = E[\cos(t) - \cos(t-\tau)]/\tau. \tag{14}$$

Other components of the momentum are zero. The value of the quasiclassical action in Eq. (13) is

$$\begin{aligned} S_{\rm st}(t,\tau) &= \frac{1}{2}\int_{t-\tau}^{t} dt''(\mathbf{p}_{st} - \mathbf{A}(t''))^2 \\ &= (I_p + U_p)\tau - 2U_p[1-\cos(\tau)]/\tau - U_p C(\tau) \\ &\quad \times \cos(2t-\tau). \end{aligned} \tag{15}$$

with

$$C(\tau) = \sin(\tau) - 4\sin^2(\tau/2)/\tau. \tag{16}$$

Finally, the first factor in the integral over τ in Eq. (13), $(\pi/\epsilon + i\tau/2)^{3/2}$ with infinitesimal ϵ, comes from the regularized Gaussian integration over $\mathbf{p}$ around the saddle-point. It expresses the effects of quantum diffusion (the spread of the electronic wave packet deposited to the continuum) and cuts off the contributions from return times τ much larger than a laser cycle.

The integral over τ in Eq. (13) can also be calculated using the saddle-point method, as will be shown in Sec. IV. However, it is worth mentioning here that Eq. (13) shows a further relation between our quantum theory and the semiclassical model of Refs. [8,9]. Indeed, in the limit $I_p \ll U_p$, the saddle point of the integral over τ in Eq. (13) tends to the stationary point $\tau = \tau_{\rm st}$ of the classical action $S_{\rm st}(t,\tau) = \int_{t-\tau}^{t} dt''(\mathbf{p}_{\rm st} - \mathbf{A}(t''))^2/2$ [Eq. (15)]. One can easily see that this point corresponds to the zero value of the initial velocity, $v(t-\tau) = p_{\rm st}(t,\tau) - A(t-\tau) = 0$. Thus, the second basic assumption of the semiclassical two-step model is justified in our theory: the electrons which contribute most to harmonic generation are not only those which return to the nucleus, but also those which appear with zero initial velocity.

The close relationship between our quantum theory and the semiclassical picture of Refs. [8,9] becomes even more striking when the harmonic emission spectrum is calculated. The spectrum is given by the Fourier transform of $x(t)$, and can also be analyzed by using the stationary phase method. It turns out that the stationary point of the fast oscillating phase in the Fourier integrand is determined by the energy conservation law: $(p_{\rm st}(t,\tau) - A(t))^2/2 + I_p = 2M+1$. Physically, it means that the $(2M+1)$-th harmonic is emitted only at those instants t at which the electrons returning to the nucleus have appropriate kinetic energy. This conclusion justifies the last basic assumption of the semiclassical model.

Since $S_{\rm st}(t,\tau)$ is a linear function of $\sin(2t)$ and $\cos(2t)$, the Fourier components of $x(t)$ can be calculated exactly. Let us introduce the Fourier components of the product of the dipole moments at t and t' and the field at t' as

$$d_x^*(p_{\rm st}(t,\tau) - A_x(t))d_x(p_{\rm st}(t,\tau) - A_x(t-\tau))E\cos(t-\tau) = \sum_M b_M(\tau)e^{-(2M+1)it}. \tag{17}$$

Owing to the properties of the dipole matrix elements due to the central symmetry of the atomic potential, all even Fourier components on the right-hand side of the above expression vanish. Typically $b_M(\tau)$ decreases quite rapidly with $|M|$ (for instance, in the case of the broad Gaussian model discussed in Sec. III, b_M's are nonzero for $M = 0, \pm 1, -2$ only).

The final formula for the $(2K+1)$-th Fourier component of $x(t)$ reads as

$$\begin{aligned} x_{2K+1} = i\sum_{M=0}^{\infty}\int_0^{\infty} d\tau \left(\frac{\pi}{\epsilon + i\tau/2}\right)^{3/2} \\ \times e^{-iF_0(\tau)} b_{K-M}(\tau) J_M(U_p C(\tau))(i)^M e^{iM\tau} \end{aligned} \tag{18}$$

where $F_0(\tau) = (U_p + I_p)\tau - 2U_p[1-\cos(\tau)]/\tau$. The integration over τ in Eq. (18) is complicated and can be performed either numerically or by using a saddle-point method (see Sec. IV). A lot of insight, however, can be drawn already from the analysis of the function $2|C(\tau)|$ which is shown in Fig. 1 (solid line). $2C(\tau)$ determines the variation of $S_{\rm st}(t,\tau)$ as a function of t. Since the action is the integral of the kinetic energy $E_{\rm kin}(t'')$ plus I_p over t'', the maxima of $2C(\tau)$ correspond therefore to the maxima of the kinetic-energy gain of the electron at t, $E_{\rm kin}(t) - E_{\rm kin}(t-\tau) = (p_{\rm st}(t,\tau) - A(t))^2/2 - (p_{\rm st}(t,\tau) - A(t-\tau))^2/2$. The dashed line in Fig. 1 represents this gain in kinetic energy, calculated by using the classical Newton equation for the case when the electron appears in the continuum with zero initial energy at the moment $t-\tau$ and revisits the nucleus at t. The two curves, classical $\Delta E_{\rm kin}/U_p$ and quantum $2|C(\tau)|$ (resulting from integration over all initial momenta p) are remarkably similar and have both maxima and zeros at the same values of τ. Moreover, the values of the maxima are the same.

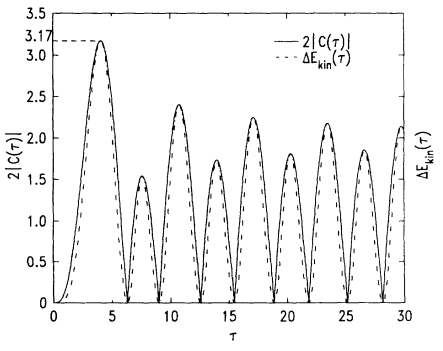

FIG. 1. The function $2|C(\tau)|$ (solid line) and the kinetic-energy gain $\Delta E_{\rm kin}(\tau)$ (dashed line) as a function of the return time τ. Note that both functions have the same extrema at the same values of τ.

As we see from Fig. 1, both functions have several maxima. They correspond to trajectories of the electron that contain one, two, or more returns to the vicinity of the nucleus (with the last one at t). The first maximum appears at $\tau_{\rm ext} \simeq 4.08$ and $2|C(\tau_{\rm ext})| \simeq 3.17$. The following maxima are between 2 and 2.4. Since the Bessel function $J_K(x)$ becomes exponentially small when $K > x$, from Eq. (18) we conclude that the absolute cutoff of HG for $U_p \gg I_p$ is at $N_{\rm max} = 2K_{\rm max} + 1 \simeq 2|C(\tau_{\rm ext})|U_p \simeq 3.17U_p$. In the range of $2.4U_p \leq 2K \leq 3.17U_p$, only the contributions from the trajectories that contain one return are relevant. As we shall see in Sec. IV, there are typically two such trajectories that correspond to two different values of τ. When $2K$ becomes smaller than $\sim 2U_p$ more and more maxima of $2|C(\tau)|$ contribute, giving rise to a more complex interference structure.

Physically, the quantum interference results from the existence of more than one possible trajectory that leads to the same final state. In particular, it becomes more and more complex as the number of trajectories returning to the nucleus several times grows. Obvioulsy, when I_p is comparable to U_p, the effects of the atomic potential on these secondary returns can be very significant. Electron rescattering will dramatically affect the phases accumulated along those trajectories and will destroy the interference patterns due to multiple returns. Note, however, that even if multiple returns are not possible because of scattering on the atomic potential, due to the existence of two trajectories with a single return the quantum interference between them is unavoidable.

III. HARMONIC SPECTRA FOR VARIOUS ATOMIC POTENTIALS

In this section, we present specific results for harmonic spectra and harmonic strengths that follow from our theory. We consider and compare results for various models of atomic potentials and ground state wave functions. This section is divided into several subsections in which we discuss a Gaussian model, the same model within the saddle-point approximation, a broad Gaussian limit, and hydrogenlike atoms. Section III E deals with the role of electron rescattering processes in which the electron returning to the nucleus is scattered away instead of being recombined. Section III F discusses the efficiency of harmonic emission for various laser frequencies.

A. Gaussian model

We assume that the ground-state s-wave function can be written in the form

$$\Psi(\mathbf{x}) = \left(\frac{\alpha}{\pi}\right)^{3/4} e^{-\alpha \mathbf{x}^2/2}, \tag{19}$$

where α is a parameter of the order of I_p. There are several models for which Eq. (19) applies. They all, however, correspond to short-range potentials that describe negative ions. First of all, we can consider a truncated harmonic-oscillator potential

$$V(\mathbf{x}) = \frac{\alpha^2 \mathbf{x}^2}{2} - \beta, \tag{20}$$

for $|\mathbf{x}| \leq \sqrt{2\beta/\alpha^2}$ and $V(\mathbf{x}) = 0$ otherwise. Here β is another parameter of the order of I_p. If β is large enough, the ground-state wave function for a potential (20) takes approximately the form (19). The ground-state energy is then $-I_p = -\beta + 3\alpha/2$. It is worth stressing, however, that Gaussian wave functions approximate well ground states of other short-range potentials, such as the screened Coulomb potential discussed in Ref. [34].

Since we are interested in transitions to and from highly energetic states in the continuum, it is safe to assume that electronic wave functions in the continuum can be described as plane waves. The dipole matrix element takes also a Gaussian form,

$$\mathbf{d}(\mathbf{p}) = i\left(\frac{1}{\pi\alpha}\right)^{3/4} \frac{\mathbf{p}}{\alpha} e^{-\mathbf{p}^2/2\alpha}. \tag{21}$$

Note the characteristic proportionality of $\mathbf{d}(\mathbf{p})$ to $\mathbf{p}$ which is universal if we consider transitions from s states.

An appealing side of the Gaussian model is that it allows us to evaluate the integral over $\mathbf{p}$ in Eq. (8) analytically. After tedious, but elementary calculations, we obtain the harmonic strengths

$$\begin{aligned} x_{2K+1} = \left(\frac{U_p}{\pi\alpha}\right)^{3/2} \frac{2(i)^{K+1}}{\alpha^2} \int_0^\infty d\tau \left(\frac{\pi}{1/\alpha + i\tau/2}\right)^{3/2} \exp[-iF_K(\tau)] \\ \times \{B(\tau) J_{K+2}(U_p C(\tau)) + i[B(\tau)e^{i\tau} + D(\tau)] J_{K+1}(U_p C(\tau)) \\ + [B(\tau) + D(\tau)e^{i\tau}] J_K(U_p C(\tau)) - iB(\tau)e^{i\tau} J_{K-1}(U_p C(\tau))\}, \end{aligned} \tag{22}$$

where the functions $B(\tau)$, $C(\tau)$, $D(\tau)$, and $F_K(\tau)$ are given in Appendix A. Note that Eq. (22) describes x_{2K+1} in the units in which the laser frequency is one. In order to express harmonic strengths in atomic units one has to multiply x_{2K+1} by the factor $\sqrt{I_p/|E_0|}$, where E_0 is the ground-state energy in a.u.

The above results are now compared with approximated formulas that make use of the saddle-point integration over $\mathbf{p}$.

B. Gaussian model and saddle-point technique

When α is large enough (which, in fact, is usually the case) we expect that the saddle-point integration over $\mathbf{p}$ should give a reasonable approximation to the expressions (22) and (A1)–(A4). In fact, the harmonic strengths when calculated with this method are given by the same expression as Eq. (22) except that this time the functions $B(\tau)$, $C(\tau)$, $D(\tau)$, and $F_K(\tau)$ take a different form (see Appendix A).

C. Broad Gaussian limit

Finally, it is interesting to note that in the limit of large α, Eqs. (A5)–(A8) may be even more simplified. To this end, we let formally $\alpha \to \infty$ and keep only the leading terms. The result for the harmonic strength again has the form (22) and the functions $B(\tau)$ and $C(\tau)$ are the same as the ones defined in Eqs. (A6) and (A7), respectively. The other functions can be found in Appendix A.

The expression (22) in the broad Gaussian limit have been used by us in Ref. [7]. It is interesting to compare the results from the three approaches discussed above which we denote by GEX (for the exact Gaussian model), GSP (for the Gaussian model with saddle-point approximation), and GBR (for the broad Gaussian limit). In Fig. 2, we present spectra obtained from the three corresponding sets of expressions. These models give similiar results. For moderate harmonic orders (in the middle of the plateau), GBR, GSP, and GEX are practically indistinguishable. For high harmonic orders, GSP and GEX are indistinguishable. Both of them give results smaller than GBR, since they account for the energy dependence of the dipole matrix element (21) that falls off slowly as the energy increases. GBR, however, produces the same kind of spectra as the other two, except for a global shift towards higher harmonic strengths by a factor slowly changing with the harmonic order.

This is a very general property of our theory. In any of its realizations (GBR, GSP, or GEX), it produces the same spectral shape except for a slowly varying energy dependent factor. The same is also true for individual harmonic strengths. They follow the same intensity dependences in the three cases, except for a constant factor, which is almost independent of the laser intensity. Macklin [35] compared the results from our theory with the exact results obtained for the zero-range potential [13]. He obtained a very good agreement for the intensity dependences of the high harmonics (but with a difference in absolute value).

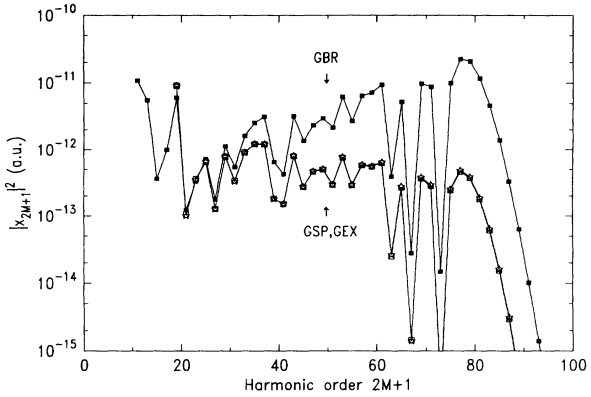

FIG. 2. Comparison of harmonic spectra obtained with GEX (open squares), GSP (stars), and GBR (black squares) methods; $I_p = 13.6$, $U_p = 20$, $\alpha = 2I_p$.

D. Hydrogenlike atoms

It is a little more difficult to calculate harmonic spectra for hydrogenlike atoms. In this case, the ground state s-wave function takes the form

$$\Psi(\mathbf{x}) = \left(\frac{\alpha^{3/4}}{\pi^{1/2}}\right) e^{-\sqrt{\alpha}|\mathbf{x}|}, \tag{23}$$

where this time $\alpha = 2I_p$. Again, since we consider transitions to and from the highly energetic continuum states, it is legimate to treat continuum states as plane waves, even though the Coulomb potential is a long-range one. The dipole matrix element takes in this case the form [36]

$$\mathbf{d}(\mathbf{p}) = i\left(\frac{2^{7/2}\alpha^{5/4}}{\pi}\right)\frac{\mathbf{p}}{(\mathbf{p}^2+\alpha)^3}. \tag{24}$$

After rather technical calculations, we obtain the following expression for the harmonic strengths:

$$x_{2K+1} = \left(\frac{128U_p^{3/2}\alpha^{5/2}}{\pi^2}\right)(i)^{K+1}\sum_{S=-\infty}^{+\infty}\int_0^\infty d\tau\left(\frac{\pi}{\epsilon+i\tau/2}\right)^{3/2}\exp[-iF_K(\tau)]$$
$$\times (i)^{-S}e^{-i\tau S}\left[iB_S(\tau)J_{K+1-S}(U_pC(\tau)) + e^{i\tau}B_S(\tau)J_{K-S}(U_pC(\tau))\right], \tag{25}$$

In Appendix B, we explain how analytic formulas for the coefficients $B_S(\tau)$ can be derived by performing an integration in the complex plane. The functions $C(\tau)$ and $F_K(\tau)$ are given in Appendix A by Eqs. (A9) and (A10), respectively. We compare the results for the hydrogenlike atoms with those for the Gaussian model in Fig. 3. The 35th harmonic strengths calculated from GBR and from expression (25) are plotted as a function of intensity in a logarithmic scale. As we see, apart from a constant absolute factor, both curves follow a similar intensity dependence and interference pattern. The change of slope in both curves corresponds to the intensity at which the 35th harmonic enters the plateau region. It determines the location of the cutoff at this particular intensity (for discussion see [7]). Note that the cutoff location for hydrogen is shifted downwards in comparison to the Gaussian model, since the 35th harmonic reaches it at a higher intensity. An explanation for this effect is presented in Sec. IV.

E. Electron rescattering

One of the important problems connected with the present theory deals with rescattering of the electrons

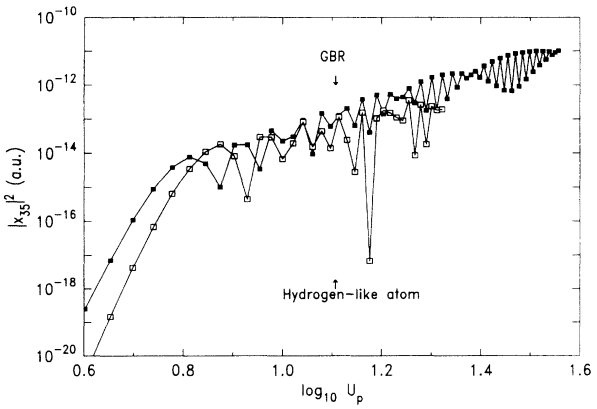

FIG. 3. Comparison of intensity dependences of the 35th harmonic for the GBR model and for a hydrogenlike atom; $I_p = 13.6$, $\alpha = 2I_p$.

that return back to the nucleus. Such processes have been estimated [9] to be quite efficient. Our theory does not include them since we have completely neglected the part of the C-C matrix elements that is responsible for those processes. We have only taken into account the part of the C-C matrix elements that describes the motion of the free electron in the field. On the other hand, the part of the C-C elements that we treat exactly does describe the spread of the wave packet accurately. This is, of course, another process which decreases quite significantly the probability for the electron to recombine after more than one return to the nucleus.

A simple way of investigating the importance of electron rescattering is to limit the integration over τ in Eqs. (8), (13), or (22) to $\tau \leq 2\pi$. Thus we account only for the trajectories such that the electron returns to the nucleus only once at time t. We eliminate all possibilities of multiple returns, which are not likely for typical experimental parameters ($\omega \sim 1 - 2$ eV, $I_p \sim 20$ eV, $I \sim 10^{14} - 10^{15}\mathrm{W/cm^2}$).

The influence of electron rescattering effects is illustrated in Figs. 4(a) and 4(b), which show results obtained using GBR for the Gaussian model and the expression (25) for the hydrogenlike atom. We compare here two curves: one with the integration range for τ unrestricted and one with the range restricted to 2π. The results in both cases are very similar and thus very encouraging, because they clearly show that indeed the major contributions to HG come from the electron trajectories that contain one and only one return to the nucleus. The contributions from those trajectories give slightly more pronounced interference patterns, but otherwise they are in a very good agreement with the more rigorous results.

In summary, we see that quantum diffusion effects alone eliminate to a great extent the impact of trajectories with multiple returns. In other words, spreading of the electron wave packet in the continuum leads to a strong decrease in the emission efficiency. One might say that although our theory formally does not take into account electron rescattering processes, it gives almost the same results as if it would. Note that the role of quantum diffusion has also been stressed in Refs. [37,38]

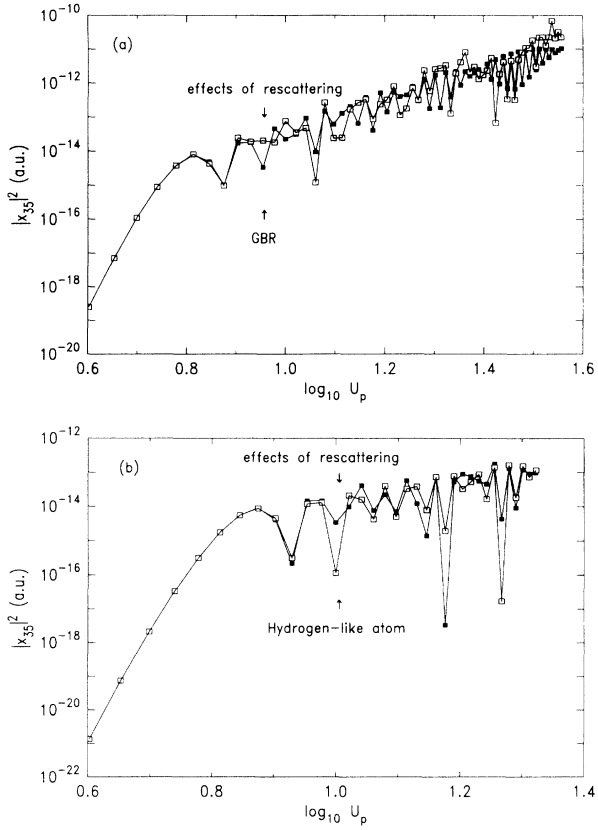

FIG. 4. (a) Comparison of intensity dependences of the 35th harmonic as for the GBR model with (black squares) and without (open squares) taking into account effects of electron rescattering (these effects are included by restricting the integration over return time τ to one optical cycle). (b) Same as (a) for a hydrogenlike atom; $I_p = 13.6$, $\alpha = 2I_p$.

F. Harmonic efficiency

High harmonics can be used as a source of coherent short-wavelength radiation. Therefore the efficiency of harmonic generation is a very important issue. One possible parameter which can be varied to optimize the harmonic efficiency is laser frequency. Using the model described above one can study the effects of laser frequency on the harmonic intensity.

Let us assume that we are interested in the emission at some fixed frequency Ω_0, and let us take $\Omega_0 \sim 50$ eV for the sake of argument. We can obtain this radiation as the 49 harmonic of 1064-nm laser light or as the 25 harmonic of 532-nm laser light. The question is in what case the harmonic intensity will be higher?

According to the cutoff rule [6] $\Omega_{\max} = I_p + 3U_p$, for a given atom and a given intensity, (e.g., close to the saturation intensity of tunneling ionization) the length of the plateau in the case of 532-nm light will be shorter owing to smaller ponderomotive potential. Obviously, if the frequency Ω_0 we are interested in is not in the plateau region for the higher incident laser frequency, it is better to use lower frequency. However, if Ω_0 is within the plateau region in both cases, in general we will be better of using shorter wavelength laser. There are two reasons for

that. First, the *number* of harmonic we have to produce to get Ω_0 is lower for higher laser frequency. Second, for higher laser frequency the laser period is shorter. Therefore, the spreading of the wave packet before the moment of re-encounter with the nucleus is smaller. As we have seen in the previous subsection, this is a very dramatic effect which strongly reduces the intensity of emission due to electron-parent ion collision. Indeed, the wave packet spreads as $\tau^{3/2}$, and for the harmonic intensity this factor should be squared.

We performed calculations for $I_p = 24$ eV and laser frequencies 1 and 2 eV, at intensities around 10^{15} W/cm^2 and harmonic frequencies around 50 eV. In all calculations the harmonic intensities were 1–2 orders of magnitude higher for 2-eV laser light than for 1-eV light. For these laser frequencies the effect of spreading alone will give only a factor of $2^3 = 8$ advantage to the shorter wavelength laser. Therefore, the fact that the harmonic *number* we need to obtain the given radiation frequency is lower for shorter wavelength is also quite important.

Summarizing, shorter wavelength radiation can be significantly more efficient for generating harmonic radiation at a given, not very high, frequency. This conclusion is consistent with experimental data [2].

IV. SADDLE-POINT ANALYSIS AND THE EXACT CUTOFF LAW

The main aim of this section is the derivation of the exact quantum cutoff law in the limit $U_p \to \infty$, with $I_p/2U_p$ constant, but smaller than one. In the semiclassical picture of Ref. [9] the cutoff law results from the energy conservation principle. One calculates the maximal kinetic energy of the electrons born at the origin with zero velocity and returning to the origin. This maximal kinetic energy turns out to be $3.17U_p$. One argues then that the maximal energy of the photons emitted due to recombination is $I_p + 3.17U_p$. Obviously, in quantum case, this picture cannot be exactly valid because of quantum tunneling and diffusion effects. First of all, in the quantum theory, the tunneling electrons are not born at the origin, but rather at x_0 such that $I_p = Ex_0\cos(t-\tau)$. When they return to x_0 with $E_{\rm kin} = 3.17U_p$, they may thus acquire an additional kinetic energy as they move from x_0 to the origin. Moreover, the electrons are not localized in the quantum case, due to the finite size of the ground-state wave function and to quantum diffusion effects. The "additional" kinetic-energy gain therefore has to be averaged over all electron trajectories. As we shall see below, the exact quantum cutoff law actually differs slightly from $I_p + 3.17U_p$.

In order to derive the quantum cutoff law, we shall examine the asymptotic behavior of Eqs. (8) and (18) in the limit when U_p, I_p, and K are large. The Fourier components of $x(t)$ are defined as

$$x_{2K+1} = \frac{1}{2\pi}\int_{t_0}^{t_0+2\pi} dt\, x(t)e^{(2K+1)it}. \tag{26}$$

Since we know already from Sec. III that the saddle-point technique is quite efficient in calculating the integral over $\mathbf{p}$, we apply the same technique to evaluate the remaining integrals over τ and t. This method is asymptotically exact provided U_p, I_p, and K are large enough. The saddle-point equations that arise from the derivatives of the classical action (9) take the form

$$\nabla_{\mathbf{p}} S(\mathbf{p},t,\tau) = \mathbf{x}(t) - \mathbf{x}(t-\tau) = 0, \tag{27}$$

$$\frac{\partial S(\mathbf{p},t,\tau)}{\partial \tau} = \frac{[\mathbf{p}-\mathbf{A}(t-\tau)]^2}{2} + I_p = 0, \tag{28}$$

$$\frac{\partial S(\mathbf{p},t,\tau)}{\partial t} = \frac{[\mathbf{p}-\mathbf{A}(t)]^2}{2} - \frac{[\mathbf{p}-\mathbf{A}(t-\tau)]^2}{2} = 2K+1. \tag{29}$$

The first of these equations indicates, as we already mentioned, that the only relevant electron trajectories are those where the electron leaves the nucleus at time $t-\tau$ and returns at t. Equation (28) has a somewhat more complicated interpretation. If I_p were zero, it would simply state that the electron leaving the nucleus at $t-\tau$ should have a velocity equal to zero. In reality, $I_p \neq 0$ and in order to tunnel through the Coulomb barrier the electron must have a negative kinetic energy at $t-\tau$. This condition cannot be fulfilled for real τ's, but can easily be fulfilled for complex τ's. The imaginary part of τ can then be interpreted as a tunneling time, just as it has been done in the seminal papers of Ammosov *et al.* [11]. Finally, we can rewrite the last expression (29) as

$$\frac{[\mathbf{p}-\mathbf{A}(t)]^2}{2} + I_p = E_{\rm kin}(t) + I_p = 2K+1. \tag{30}$$

This is simply the energy conservation law, which gives the final kinetic energy of the recombining electron that generates the $(2K+1)$-th harmonic.

These equations can be used to derive the cutoff law. Indeed, Eq. (30) clearly says that the maximum emitted harmonic frequency is given by the maximum possible kinetic energy the electron has at the moment t of collision with the nucleus. Qualitatively, this conclusion is fully consistent with the classical model of Refs. [8,9]. Quantitatively, there is a difference because Eqs. (27) and (28), which have to be considered together with Eq. (30), naturally account for the tunneling process and its influence on the electron kinetic energy at the moment it encounters the nucleus again.

In order to obtain the cutoff law, we must use the first two of saddle-point equations to express any two of the variables $\mathbf{p},t,\tau$ via the remaining third. Then we have to substitute the results into Eq. (30) and find the maximum of the left-hand side expression as a function of the remaining variable. In practice, it is very convenient to use the return time τ and solve Eqs. (27) and (28) for $\mathbf{p}$ and t as functions of τ. Thus, the cutoff law reads as

$$(2K+1)_{\max} = \max \mathrm{Re}\left(\frac{[\mathbf{p}(\tau)-\mathbf{A}(t(\tau))]^2}{2}\right) + I_p \tag{31}$$

under the constraint that the imaginary part of the right-

hand side expression is equal to zero.

Inserting the solution of Eq. (27), i.e. the expression for $p_{\rm st}(t,\tau)$, into Eq. (28) it is easy to solve the latter with respect to $\sin(t-\tau/2)$ and $\cos(t-\tau/2)$. Namely, Eq. (28) reduces to the form

$$\sin(t-\tau/2)a(\tau)-\cos(t-\tau/2)s(\tau)=i\sqrt{\frac{I_p}{2U_p}}, \quad (32)$$

where

$$a(\tau)=\cos(\tau/2)-\frac{2\sin(\tau/2)}{\tau}, \quad (33)$$

$$s(\tau)=\sin(\tau/2). \quad (34)$$

Note that the function $C(\tau)$, as expressed by Eq. (16), is $C(\tau)=2s(\tau)a(\tau)$. From Eq. (32), we obtain

$$\sin(t-\tau/2)=\frac{i\sqrt{\frac{I_p}{2U_p}}a(\tau)\pm s(\tau)\sqrt{s^2(\tau)+a^2(\tau)+\frac{I_p}{2U_p}}}{[s^2(\tau)+a^2(\tau)]}, \quad (35)$$

$$\cos(t-\tau/2)=\frac{-i\sqrt{\frac{I_p}{2U_p}}s(\tau)\pm a(\tau)\sqrt{s^2(\tau)+a^2(\tau)+\frac{I_p}{2U_p}}}{[s^2(\tau)+a^2(\tau)]}, \quad (36)$$

There exists also a pair of complex-conjugated solutions. The choice of the appropriate pair is dictated by the requirement that the resulting imaginary part of the classical action must be negative, so that it causes an exponential decrease of the corresponding transition amplitudes. The results do not depend on the choice of the sign in front of the square root in Eqs. (35) and (36), provided it is the same in both of them.

Inserting these solutions into Eq. (29), we obtain a closed form equation for τ,

$$8\frac{a^2(\tau)s^2(\tau)\left[s^2(\tau)+a^2(\tau)+\frac{I_p}{U_p}\right]}{(s^2(\tau)+a^2(\tau))^2}+8i\sqrt{\frac{I_p}{2U_p}}\frac{a(\tau)s(\tau)[a^2(\tau)-s^2(\tau)]\sqrt{s^2(\tau)+a^2(\tau)+\frac{I_p}{2U_p}}}{[s^2(\tau)+a^2(\tau)]^2}=\frac{2K+1}{U_p}. \quad (37)$$

Let us first consider a limiting case $I_p=0$. Eq. (37) takes then a simple form

$$8\frac{a^2(\tau)s^2(\tau)}{[s^2(\tau)+a^2(\tau)[}=\frac{2K+1}{U_p}. \quad (38)$$

The function on the left-hand side of Eq. (38) is nothing else but the classical kinetic-energy gain, $\Delta E_{\rm kin}(\tau)$, as plotted in Fig. 1 (dashed line). Equation (38) allows for real solutions (tunneling time equal to zero) provided K is not too large. In order to find out how large it can be, we have to find the maxima of $\Delta E_{\rm kin}(\tau)$. As we already learned in Sec. II, these maxima occur exactly at the same points as the maxima of the function $C(\tau)$. There are two families of maxima, corresponding to $a(\tau)=-s(\tau)$ and to $a(\tau)=s(\tau)$. The first family are the solutions of the equation

$$\tan(\tau/2)=\frac{1}{2/\tau-1}, \quad (39)$$

and contains $\pi<\tau_1<2\pi$, $\tau_3\simeq 4\pi$, etc. The first solution $\tau_1\simeq 4.08$ is the same as $\tau_{\rm ext}$ discussed in Sec. II. For this solution, the kinetic-energy gain attains the absolute maximum equal to 3.17. Further solutions give maxima in the range 2–2.4. The second family $[a(\tau)=s(\tau)]$ fulfills

$$\tan(\tau/2)=\frac{1}{2/\tau+1}, \quad (40)$$

and contains $\tau_2\simeq 3\pi$, $\tau_4\simeq 4\pi$ etc., with values of maxima also in the range 2–2.4.

For $2K+1\geq 3.17U_p$ there are no real solutions to Eq. (38). The reason is not because of the impossibility of tunneling, but rather because of the impossibility of gaining sufficiently large kinetic energy. The solutions of Eq. (38) then acquire a significant imaginary part which introduces an exponentially decreasing factor to $\exp[-iS(\mathbf{p},t,\tau)]$ at the saddle point and causes a sharp (exponential) cutoff in the harmonic spectrum. We conclude that for $I_p=0$, the cutoff occurs at $2K+1\simeq 3.17U_p$.

It is much more difficult to study the case of finite I_p. One way to do it is to perform a systematic expansion in I_p/U_p. It is easy to see, however, that the zeroth order (in I_p/U_p) solution of Eq. (28) is doubly degenerated and the corresponding saddle point is not Gaussian but rather of third order. Integration around such a saddle point gives rise to Airy functions [39] and will be discussed elsewhere. In the present paper, we shall use a simple approximation valid in the limit $I_p\ll U_q$ and a numerical evaluation in the general case, where I_p is of the order of U_p or slightly smaller.

Let us denote

$$f(\tau)=8\frac{a^2(\tau)s^2(\tau)\left[s^2(\tau)+a^2(\tau)+\frac{I_p}{U_p}\right]}{[s^2(\tau)+a^2(\tau)]^2} \quad (41)$$

$$g(\tau)=8\frac{a(\tau)s(\tau)[a^2(\tau)-s^2(\tau)]\sqrt{s^2(\tau)+a^2(\tau)+\frac{I_p}{2U_p}}}{[s^2(\tau)+a^2(\tau)]^2} \quad (42)$$

Equation (37) then takes a simple form

$$f(\tau)+i\sqrt{\frac{I_p}{2U_p}}g(\tau)=\frac{2K+1}{U_p}. \quad (43)$$

Strictly speaking the exact quantum cutoff law [see Eq. (31)] is thus

$$(2K+1)_{\rm max}=U_p\max{\rm Re}\left(f(\tau)+i\sqrt{\frac{I_p}{2U_p}}g(\tau)\right), \quad (44)$$

under the constraint that

$$\mathrm{Im}\left(f(\tau)+i\sqrt{\frac{I_p}{2U_p}}g(\tau)\right)=0. \tag{45}$$

Let us first discuss the case when $I_p \ll U_p$. We expect that the maximum of the left-hand side of Eq. (44) in this case is reached at $\tau \simeq \tau_1$, so that we may write $\tau = \tau_1 + \delta\tau_R + i\tau_I$, where both $\delta\tau_R$ and τ_I are small. The real part of τ, $\tau_1 + \delta\tau_R$ has the meaning of a return time as before, whereas the imaginary part τ_I might be interpreted as a tunneling time. Using this Ansatz and expanding $f(\tau)$ to the second order and $g(\tau)$ to the first order in $\delta\tau_R + i\tau_I$, we obtain from Eqs. (44) and (45)

$$\tau_I = -\sqrt{\frac{I_p}{2U_p}}\frac{g'(\tau_1)}{f''(\tau_1)}, \tag{46}$$

and $\delta\tau_R = 0$. The primes denote here derivatives. After complicated, but otherwise elementary calculations, we obtain the explicit form of the cutoff law for $I_p \ll U_p$,

$$\begin{aligned}(2K+1)_{\max} &\simeq 3.17U_p + I_p\left(1+\frac{s^2(\tau_1)}{s^2(\tau_1)(\tau_1-1)}\right)\\ &\simeq 3.17U_p + 1.32I_p.\end{aligned} \tag{47}$$

This result shows that the phenomenological semiclassical law $2K+1 = 3.17U_p + I_p$ is modified by the effects of quantum tunneling and quantum diffusion even for $I_p \ll U_p$. In this regime of parameters the small change of the prefactor in front of the I_p is not very important and is hardly detectable both in numerical analysis and in experiments. There are, however, quite significant differences in comparison to the phenomenological law $3.17U_p + I_p$ for $I_p \simeq O(U_p)$. In order to illustrate this point we need to consider larger values of I_p, and therefore to find the exact cutoff law from Eq. (44).

The exact evaluation of the cutoff presents no numerical difficulties. The cutoff law has a form

$$(2K+1)_{\max} = 3.17U_p + I_pF(I_p/U_p), \tag{48}$$

and the factor $F(I_p/U_p)$ is plotted in Fig. 5 as a function of I_p/U_p. As we see, $F(x) = 1.32$ for small x, in agreement with expression (47). $F(x)$ decreases slowly as x grows. In Fig. 6 we show harmonic spectra for $I_p = 30$ and $U_p = 20$ and 10. The phenomenological expression gives in those cases cuts off at $2K+1$ equal to 93 and 62, respectively. The exact quantum expression predicts them at 101 and 69. Evidently, the quantum expression is more accurate.

Physically, the shift of the cutoff energy compared to the classical picture results from two effects. (i) Since the electron must tunnel out, it cannot appear at the origin. It appears at x_0 such that $I_p = Ex_0\cos(t-\tau)$. After it comes back to x_0, it can gain an additional kinetic energy on the way towards origin, equal approximately to the work of the electric field over the interval $[x_0, 0]$, i.e., $Ex_0\cos(t)$. The cut-off law should therefore be $3.17U_p + I_p\cos(t)/\cos(t-\tau)$. Inserting the values of $\cos(t)$ and $\cos(t-\tau)$ as obtained from the saddle-point equations for $I_p = 0$, we recover the result $(2K+1)_{\max} = 3.17U_p + 1.32I_p$. (ii) The electron undergoes diffusion which tends to average and decrease the effect of the additional kinetic-energy gain for larger I_p.

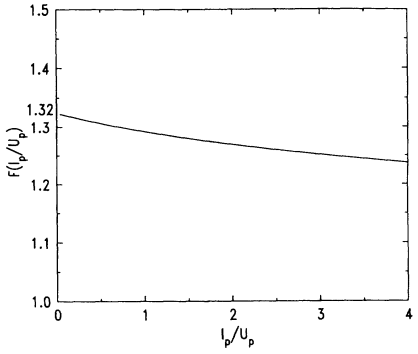

FIG. 5. Plot of the function $F(I_p/U_p)$ that enters the exact cutoff law, $(2K+1)_{\max} = 3.17U_p + I_pF(I_p/U_p)$.

The exact cutoff law is asymptotically valid when both U_p and I_p tend to infinity, so that the ratio $I_p/2U_p$ remains constant (and not too large). Strictly speaking, however, the saddle-point equations, Eqs. (27)–(29), are valid if and only if the atomic dipole moment $d(\mathbf{p}-\mathbf{A}(t-\tau))$ is not singular at the saddle point. This is the case for the Gaussian model. Unfortunately, it is not true for more realistic models for which $d(\mathbf{p}-\mathbf{A}(t-\tau))$ behaves as $\{[\mathbf{p}-\mathbf{A}(t-\tau)]^2/2 + I_p\}^{-\eta}$ with some positive exponent η (equal for instance to 3 for hydrogen). Evidently, the atomic dipole moment is singular at the saddle point. This behavior of the atomic matrix elements is the direct consequence of the asymptotic behavior of the ground-state wave function which is proportional to $\exp(-\sqrt{2I_p}r)$ for large r. Therefore, in order to be more accurate one has to incorporate the effects of the finite size of the ground-state wave function in solving the saddle-point equations. This leads to corrections to the cut-off law of the order of $U_p^{-1/4}$, which vanish as

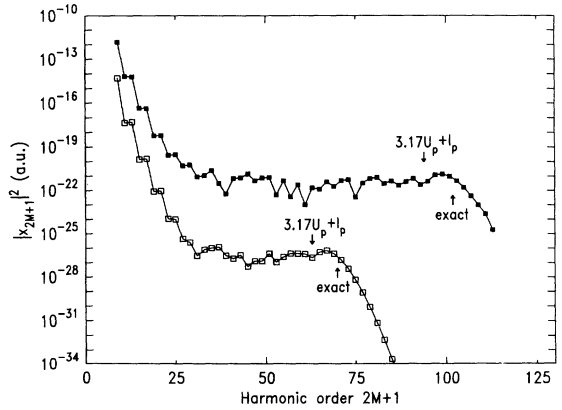

FIG. 6. Harmonic spectra for the GBR model with $I_p = 30$, $\alpha = I_p$. The curve with open squares is obtained for $U_p = 10$ and the one with black squares for $U_p = 20$. The locations of the phenomenological and exact cutoffs are indicated by the arrows.

$U_p \to \infty$, but rather slowly. These corrections counteract the cut-off shift discussed in this section and move the cutoff location to a lower energy. They are responsible for the difference in the position of the cutoff between hydrogen and the GBR model observed in Fig. 3. These points will be discussed in detail in a future publication.

V. GROUND-STATE DEPLETION

It is possible to generalize our theory to include the effect of the ground-state depletion. To this aim, we consider the Schrödinger equations,

$$\dot{a}(t) = iE\cos(t)\int d^3\mathbf{v}\; d_x(\mathbf{v})b(\mathbf{v},t), \tag{49}$$

$$\dot{b}(\mathbf{v},t) = -i\left(\frac{\mathbf{v}^2}{2}+I_p\right)b(\mathbf{v},t) - E\cos(t)\,\frac{\partial b(\mathbf{v},t)}{\partial v_x} + iE\cos(t)\,d_x(\mathbf{v})a(t). \tag{50}$$

We solve Eq. (50) and insert the solution into (49). Assuming that $a(t)$ changes slowly we can set $a(t') \simeq a(t)$. The differential equation for $a(t)$ takes the form

$$\dot{a}(t) = -\gamma(t)a(t), \tag{51}$$

where the complex rate $\gamma(t)$ is defined by,

$$\gamma(t) = \int d^3\mathbf{p}\int_0^\infty d\tau E\cos(t)d_x(\mathbf{p}-\mathbf{A}(t)) \times E\cos(t-\tau)d_x(\mathbf{p}-\mathbf{A}(t-\tau))e^{-iS(\mathbf{p},t,\tau)}. \tag{52}$$

$\gamma(t)$ is in general time dependent and becomes periodic as t grows, having maxima at the peak values of the electric field, when the electron has a much larger chance of tunneling. Equation (52) can be analyzed using the saddle point method and in the limit of $U_p \gg I_p \gg 1$, one recovers the tunneling rate obtained by Ammosov *et al.* [11]. Note, however, that our theory is more general, since it takes into account quantum interference effects and the returns of the electron to the nucleus, which are completely absent in the approach of Ref. [11]. We leave the detailed discussion of the time-dependent rate to a future publication and we limit our discussion here to the case where $\gamma(t)$ can be substituted by its time average

$$\bar{\gamma} = \lim_{t\to\infty}\frac{1}{t}\int_0^\infty dt'\,\gamma(t'). \tag{53}$$

For the Gaussian models (GEX, GSP, and GBR) the expression for $\bar{\gamma}$ takes this form,

$$\bar{\gamma} = 4\left(\frac{U_p}{\alpha}\right)^2\frac{1}{\pi\alpha^2}\int_0^\infty d\tau\left(\frac{\pi}{1/\alpha+i\tau/2}\right)^{3/2}\exp[-iF_0(\tau)] \times\{-B(\tau)J_2(U_pC(\tau)) + [B(\tau)+D(\tau)\cos(\tau)]J_0(U_pC(\tau)) + 2i[B(\tau)\cos(\tau)+D(\tau)/2]J_1(U_pC(\tau))\}, \tag{54}$$

In Fig. 7, we present the intensity dependence of $\bar{\gamma}$ as obtained from the GBR model. As we see, both the real and the imaginary parts of $\bar{\gamma}$ [see Figs. 7(a) and 7(b)] increase (in absolute value) with intensity. The real part of $\bar{\gamma}$, γ_R describes the rate of depletion of the ground state. For the laser pulse duration t_D the saturation intensity is achieved at $\bar{\gamma}_{\rm sat}t_DE \simeq 1$, i.e., when the atom is fully ionized during the interaction with the laser pulse. The imaginary part of $\bar{\gamma}$, γ_I describes a dynamical shift of the ground-state energy (not to be confused with the ponderomotive shift). It is proportional to the laser intensity and becomes quite large as $\gamma_R \simeq \bar{\gamma}_{\rm sat}$.

Taking into account the depletion, the expression for the time-dependent dipole moment takes the form

$$x(t) = i\int d^3\mathbf{p}\int_0^t d\tau d_x^*(\mathbf{p}-\mathbf{A}(t))E\cos(t-\tau)d_x(\mathbf{p}-\mathbf{A}(t-\tau))e^{-iS(\mathbf{p},t,\tau)-\bar{\gamma}^*t-\bar{\gamma}(t-\tau)}. \tag{55}$$

The Fourier transform of $x(t)$, or rather its modulus squared, now consists of a sequence of Lorentzian peaks with width $2\gamma_R$. The harmonic strengths can be calculated as the total area covered by each of these peaks (equal to the total energy radiated at the corresponding harmonic frequency).

Using Eq. (18) we obtain

$$\tilde{x}(\Omega) = \frac{i}{\sqrt{2\pi}}\sum_M\int_0^{t_D} d\tau\; b_{K-M}(\tau)J_M(U_pC(\tau))(i)^M e^{iM\tau}h(\tau,\Omega-2M-1), \tag{56}$$

where

$$h(\tau,\Omega-2M-1) = e^{\bar{\gamma}\tau}\frac{e^{-2\gamma_R\tau+i(\Omega-2M-1)\tau} - e^{-2\gamma_Rt_D+i(\Omega-2M-1)t_D}}{2\gamma_R+i(\Omega-2M-1)}. \tag{57}$$

The peaks are centered at $\Omega = 2M+1$. The harmonic strengths $|x_{2M+1}|^2$ are thus approximately equal to $|\tilde{x}(2M+1)|^2$ times a factor that accounts for the area of the peak, $2\pi\gamma_R/[1-\exp(-2\gamma_Rt_D)]$. For Gaussian models, for instance, we obtain

$$|x_{2M+1}|^2 = \frac{\gamma_R}{1-\exp(-2\gamma_R t_D)}\left|\left(\frac{U_p}{\pi\alpha}\right)^{3/2}\frac{2(i)^{M+1}}{\alpha^2}\int_0^\infty d\tau\left(\frac{\pi}{1/\alpha+i\tau/2}\right)^{3/2}\exp[-iF_M(\tau)]h(\tau,0)\right.$$
$$\times\{-B(\tau)J_{M+2}(U_pC(\tau))+i[B(\tau)e^{i\tau}+D(\tau)]J_{M+1}(U_pC(\tau))$$
$$\left.+[B(\tau)+D(\tau)e^{i\tau}]J_M(U_pC(\tau))-iB(\tau)e^{i\tau}J_{M-1}(U_pC(\tau))\}\right|^2. \quad (58)$$

A similar expression can be derived for hydrogenlike atoms.

In order to study the effects of depletion, we have first treated $\bar{\gamma}$ as a free parameter, [i.e., not determined from Eq. (53)] and we have calculated harmonic spectra for $U_p = 20$ and several values of $\bar{\gamma}$. In particular, we have performed calculations for $\gamma_I = 0$ and $\gamma_R = 0.01$ and 1. The duration time of the laser pulse was chosen to be 20 optical cycles. The spectrum for $\gamma_R = 0.01$ differs only slightly from the result obtained for $\gamma_R = 0$, even though the system is already close to saturation. A further increase of γ_R decreases the harmonic strengths quite significantly, and smoothes out the spectrum, i.e., reduces the effects of quantum interferences. The depletion does not change the cutoff location for the single-atom spectra. That can be understood since even for $\gamma_R = 1$, when the ionization takes place more or less within one optical cycle, the electron still has a chance to come back at least once to the origin.

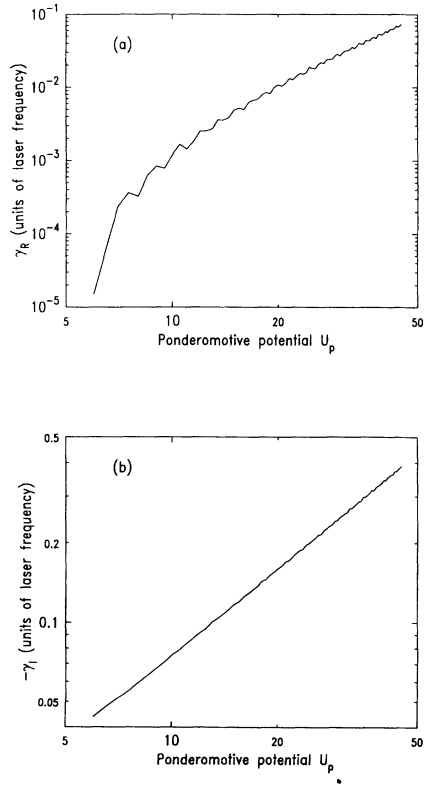

FIG. 7. Intensity dependence of the depletion rate γ_R for the GBR model; $I_p = 5$, $\alpha = 2I_p$; (b) Same as (a) for the ac-Stark shift of the ground-state energy $-\gamma_I$.

In order to study the full dynamical influence of the depletion on harmonics, we have evaluated $\bar{\gamma}$ from Eq. (54) (see Fig.7) and the harmonic strengths from Eq. (58) for the GBR model. An example for the 35th harmonic is shown in Fig. 8. Again, the main effect of the depletion consists of the decrease of the harmonic strength. For high enough intensities, the harmonic strength becomes a slowly decreasing function of the laser intensity.

It is now clear that in order to get higher *conversion efficiency* of harmonic emission one should use shorter laser pulses. Indeed, according to the results of this section and Sec.III E, the main contribution to the harmonic emission is given by the first re-encounter of the continuum electron with the nucleus, and the effects of secondary collisions are not very strong. Therefore, one can use very short—a few cycles long— laser pulses of high intensity. Even though the ground state of the atom will be depleted very fast, the electron will still be able to return to the nucleus and collide with it at least once. As a result, the absolute harmonic intensity will not decrease significantly. On the other hand, the energy of the shorter incident laser pulse will be reduced. In other words, at high intensities, when the depletion of the atom is very fast and harmonic emission occurs only at the beginning of the pulse, most of the pulse energy is wasted and using short pulses will solve this problem.

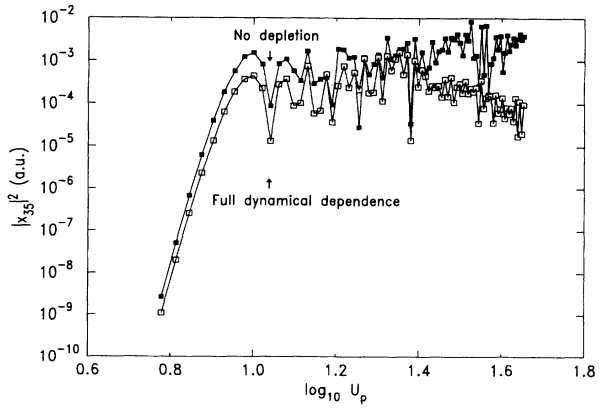

FIG. 8. Comparison of intensity dependences of the 35th harmonic with (open squares), and without (black squares) depletion. Both curves are obtained for the GBR model with $I_p = 5$, $\alpha = 2I_p$. The duration of the pulse t_D is taken to be 50 optical cycles.

VI. CONCLUSION

In summary, we would like to point out the important aspects of our theoretical formulation and in particular how it complements both the exact quantum-mechanical calculations of [6] and the semiclassical calculations presented in Refs. [8,9].

The formulation exposed in this work allows us to derive analytically the cutoff law determined by extensive numerical calculations [6] and interpretated with semiclassical arguments [8,9]. In fact, this derivation gives an expression very close numerically but slightly more complicated than the linear formula $3.17U_p + I_p$, as discussed in Sec. IV.

Our approach provides a description of HG into two steps, as is also done in Refs. [8,9]. However, we do not assume as in Ref. [9] that the electron appears near the origin with a zero velocity. As always in quantum mechanics, we deal with amplitudes describing processes in which the electron has any initial velocity and initial position. It is the result of the theory that shows, rigorously, that the main contribution to HG comes from the electrons that appear at the nucleus with a velocity close to zero, and return to it. Thus, we present here a quantum-mechanical justification of the two-step semiclassical picture. In other words, we demonstrate that the problem of coherent control of HG indeed reduces to the problem of the laser control over classical electron trajectories.

Our approach allows for a simple analysis of harmonic efficiency as a function of different laser and atomic parameters, such as laser frequency, pulse duration, and atomic ionization potential. According to our results, radiation at a given frequency can be obtained with higher efficiency by using shorter laser pulses of higher frequency.

This theory is very similar to the one developed in Ref. [13] but it is not restricted to a zero range potential. We can describe hydrogenlike atoms and account for electron rescattering processes (as we did in Sec. III). The effects of the Coulomb potential, introducing corrections to the classical action could be included as in Ref. [11]. We can also investigate the influence of the ground-state depletion on the high harmonic production and on the cutoff formula (see Sec. V).

Finally, we should emphasize that the approach developed in the present paper for a linearly polarized monochromatic laser field can easily be generalized to laser fields of arbitrary, and in particular time-dependent, ellipticity or to multicolor laser fields. Moreover, in order to make a realistic comparison with the experimental data one has to take into account propagation effects. Our theory provides a relatively easy way of calculating the single atom response in a very general situation. The results can be used as an input to the propagation equations.

ACKNOWLEDGMENTS

We are grateful to K. C. Kulander, K. J. Schafer, and S. Geltman for helpful discussions. One of us (M.L.) thanks the SPAM in Saclay and JILA in Boulder for hospitality and for financial support.

APPENDIX A

In this appendix, we present the explicit expressions for the functions $C(\tau)$, $B(\tau)$, $D(\tau)$, and $F_K(\tau)$ that enter the expression (22). For the exact Gaussian model (GEX), we obtain

$$C(\tau) = \sin(\tau) - \frac{2i}{\alpha}\cos(\tau) + \frac{2i}{(1/\alpha + i\tau/2)} \times \left(\frac{\cos(\tau/2)}{\alpha} + i\sin(\tau/2)\right)^2, \tag{A1}$$

$$B(\tau) = -\frac{1}{2(1/\alpha + i\tau/2)^2}\left(\frac{\cos(\tau/2)}{\alpha} + i\sin(\tau/2)\right)^2 + \frac{\cos(\tau/2)}{(1/\alpha + i\tau/2)}\left(\frac{\cos(\tau/2)}{\alpha} + i\sin(\tau/2)\right) - \frac{1}{2}, \tag{A2}$$

$$D(\tau) = -2B(\tau) - 1 + \cos(\tau) + \frac{1}{4(1/\alpha + i\tau/2)U_p}, \tag{A3}$$

and, finally,

$$F_K(\tau) = (I_p + U_p - K)\tau - \frac{2iU_p}{\alpha} + \frac{2iU_p}{(1/\alpha + i\tau/2)} \times \left(\frac{\cos(\tau/2)}{\alpha} + i\sin(\tau/2)\right)^2. \tag{A4}$$

Obviously, the function $C(\tau)$ is an analog of the function $C(\tau)$ from Fig. 1, which is why we denote them in the same way. For the Gaussian model treated with the help of saddle point method (GSP), we get

$$C(\tau) = \sin(\tau) - \frac{2i}{\alpha}\cos(\tau) - \frac{4\sin^2(\tau/2)}{\tau}\left(1 + \frac{2i}{\tau\alpha}\right) + 4i\frac{\sin\tau}{\tau\alpha}, \tag{A5}$$

$$B(\tau) = -\frac{2\sin^2(\tau/2)}{\tau^2} + \frac{\sin(\tau)}{\tau} - \frac{1}{2}, \tag{A6}$$

$$D(\tau) = -2B(\tau) - 1 + \cos(\tau), \tag{A7}$$

and

$$F_K(\tau) = (I_p + U_p - K)\tau - \frac{2iU_p}{\alpha} - \frac{4U_p\sin^2(\tau/2)}{\tau}\left(1 + \frac{2i}{\alpha\tau}\right) + \frac{4iU_p\sin(\tau)}{\alpha\tau} \tag{A8}$$

Finally, in the broad Gaussian limit (GBR), the functions $B(\tau)$ and $D(\tau)$ are the same as the ones defined in Eqs. (A6) and (A7), respectively. Other functions are given by

$$C(\tau) = \sin(\tau) - \frac{4\sin^2(\tau/2)}{\tau}, \tag{A9}$$

$$F_K(\tau) = (I_p + U_p - K)\tau - \frac{4U_p\sin^2(\tau/2)}{\tau}. \tag{A10}$$

APPENDIX B

The coefficients $B_S(\tau)$ that enter Eq. (25) are defined as

$$B_S(\tau) = \int_0^{2\pi} \frac{dt}{2\pi} e^{2Sit} \frac{[p_{st}(t,\tau) - A(t)][p_{st}(t,\tau) - A(t-\tau)]}{\{[p_{st}(t,\tau) - A(t)]^2 + \alpha\}\{...\}^3\{[p_{st}(t,\tau) - A(t-\tau)]^2 + \alpha'\}^3} \tag{B1}$$

where $\alpha = \alpha' = 2I_p$. Introducing a new variable $z = \exp(-2it)$ we obtain

$$B_S(\tau) = \int_C \frac{dz}{2\pi i} H(z), \tag{B2}$$

where the integral runs around the unit circle along the contour C. The function $H(z)$ is given by

$$H(z) = \frac{z^{S+5} W_3(z)}{[W_1(z)W_2(z)]^3}, \tag{B3}$$

and the quadradic polynomials $W_i(z)$, $i = 1, 2, 3$, take the form

$$W_1(z) = U_p[s(\tau) - ia(\tau)]^2 e^{-i\tau} z^2 + \left\{U_p[s^2(\tau) + a^2(\tau)] + \alpha\right\} z + U_p[s(\tau) + ia(\tau)]^2 e^{i\tau}, \tag{B4}$$

$$W_2(z) = U_p(s(\tau) + ia(\tau))^2 e^{-i\tau} z^2 + \left\{U_p[s^2(\tau) + a^2(\tau)] + \alpha'\right\} z + U_p[s(\tau) - ia(\tau)]^2 e^{i\tau}, \tag{B5}$$

$$W_3(z) = U_p[s(\tau) + a^2(\tau)]\left(e^{-i\tau} z^2 + 2z + e^{i\tau}\right). \tag{B6}$$

The function $H(z)$ has two singularities inside the contour C. These are

$$z_1 = -\frac{2(s^2 + a^2) + \alpha/U_p - \sqrt{(\alpha/U_p)^2 + 4(s^2 + a^2)\alpha/U_p}}{2(s + ia)^2} e^{i\tau}, \tag{B7}$$

$$z_2 = -\frac{2(s^2 + a^2) + \alpha'/U_p - \sqrt{(\alpha'/U_p)^2 + 4(s^2 + a^2)\alpha'/U_p}}{2(s - ia)^2} e^{i\tau}. \tag{B8}$$

At these points, the function $H(z)$ has poles of third order at least. Using Cauchy's theorem, we obtain analytic expressions for the coefficients $B_S(\tau)$ as

$$B_S(\tau) = \frac{1}{2} \sum_{i=1,2} \lim_{z \to z_i} \frac{d^2}{dz^2} \left[(z - z_i)^2 H(z)\right]. \tag{B9}$$

Strictly speaking expression (B9) is valid only if the two poles are not degenerated, i.e., $z_1 \neq z_2$. Unfortunately for the values of τ when either $s(\tau)$ or $a(\tau)$ vanish that is not the case. The singularity is then of the sixth order and the calculations become very tedious. In numerical calculations, it is very convenient to solve this problem by using $\alpha \neq \alpha'$, at least in the vicinity of $\tau's$ for which $z_1 = z_2$. For α, α' of the order of 20, it is enough to set the difference between them to about one to assure a good convergence of the results.

[1] See *Proceedings of the Workshop, Super Intense Laser Atom Physics (SILAP) III*, edited by B. Piraux (Plenum Press, New York, in press).

[2] S. Watanabe, K. Kondo, and Y. Nabekawa (unpublished).

[3] C. Rhodes, Phys. Scr. **T17**, 193 (1987); K. Boyer, R. Rosman, G. Gibson, H. Jara, T. Luk, I. McIntyre, A. McPerson, J. Solem, and C. Rhodes, J. Opt. Soc. Am. B **5**, 1237 (1988).

[4] A. L'Huillier and Ph. Balcou, Phys. Rev. Lett. **70**, 774 (1993).

[5] J. J. Macklin, J. D. Kmetec, and C. L. Gordon III, Phys. Rev. Lett. **70**, 766 (1993).

[6] J. L. Krause, K. J. Schafer, and K. C. Kulander, Phys. Rev. Lett. **68**, 3535 (1992).

[7] A. L'Huillier, M. Lewenstein, P. Salières, Ph. Balcou, J. Larsson, and C. G. Wahlström, Phys. Rev. A **48**, R3433 (1993).

[8] K. C. Kulander, K. J. Schafer, and J. L. Krause, in *Proceedings of the Workshop , Super Intense Laser Atom Physics (SILAP) III* (Ref. [1]).

[9] P. B. Corkum, Phys. Rev. Lett. **71**, 1995 (1993).

[10] L. V. Keldysh, Zh. Eksp. Teor. Fiz. **47**, 1945 (1964) [Sov. Phys. JETP **20**, 1307 (1965)]; F. Faisal, J. Phys. B **6**, L312 (1973); H. R. Reiss, Phys. Rev. A **22**, 1786 (1980).

[11] M. V. Ammosov, N. B. Delone, and V. P. Kraĭnov, Zh. Eksp. Teor. Fiz. **91**, 2008 (1986) [Sov. Phys. JETP **64**, 1191 (1986)]; N. B. Delone and V. P. Kraĭnov, J. Opt. Soc. Am. B **8**, 1207 (1991); V. P. Kraĭnov and V. M. Ristić, Zh. Eksp. Teor. Fiz. **101**, 1479 (1992) [Sov. Phys. JETP **74**, 789 (1992)].

[12] M. Yu. Ivanov, P. B. Corkum, P. Dietrich, and N. Burnett, in Proceedings of the Sixth International Conference of Multiphoton Processes, Quebec, 1993 (unpublished).

[13] W. Becker, S. Long, and J. K. McIver, Phys. Rev. A **41**, 4112 (1990).

[14] A. L'Huillier, Ph. Balcou, S. Candel, K. J. Schafer, and K. C. Kulander, Phys. Rev. A **46**, 2778 (1992).

[15] K. C. Kulander and B. W. Shore, Phys. Rev. Lett. **62**, 524 (1989).

[16] J. H. Eberly, Q. Su, and J. Javanainen, Phys. Rev. Lett.

62, 881 (1989).
[17] S. Chelkowski, T. Zuo, and A. D. Bandrauk, Phys. Rev. A **46**, R5342 (1992); see also Ref. [22].
[18] V. C. Reed and K. Burnett, Phys. Rev. A **46**, 424 (1992).
[19] R. M. Potvliege and R. Shakeshaft, Phys. Rev. A **40**, 3061 (1989).
[20] B. Sundaram and P. W. Milonni, Phys. Rev. A **41**, 6571 (1990).
[21] L. Plaja and L. Roso-Franco, J. Opt. Soc. Am. B **9**, 2210 (1992); see also Ref. [1].
[22] A. E. Kaplan and P. L. Shkolnikov, in Proceedings of the Sixth International Conference on Multiphoton Processes, Quebec, 1993 (unpublished).
[23] K. C. Kulander and B. W. Shore, J. Opt. Soc. Am. B **7**, 502 (1990); see also K. C. Kulander and K. J. Schafer, in Proceedings of the Sixth International Conference on Multiphoton Processes, Quebec, 1993 (unpublished).
[24] M. Yu. Ivanov and P. B. Corkum, Phys. Rev. A **48**, 580 (1993); M. Yu. Ivanov, P. B. Corkum, and P. Dietrich, Laser Phys. **3**, 375 (1993).
[25] G. Bandarage, A. Maquet, T. Ménis, R. Taïeb, V. Véniard, and J. Cooper, Phys. Rev. A **46**, 380 (1992).
[26] Th. Auguste, P. Monot, L. A. Lompré, G. Mainfray, and C. Manus, J. Phys. B **25**, 4181 (1992).
[27] E. Mevel, P. Breger, R. Trainham, G. Petite, P. Agostini, A. Migus, J.-P. Chambaret, and A. Antonetti, Phys. Rev. Lett. **70**, 406 (1993).
[28] M. H. Mittleman, *Introduction to Theory of Laser-Atom Interactions* (Plenum, New York, 1982).
[29] See, for instance, the contribution of H. R. Reiss to Ref. [1].
[30] M. Lewenstein, J. Mostowski, and M. Trippenbach, J. Phys. B **18**, L461 (1985); J. Grochmalicki, J. R. Kukliński, and M. Lewenstein, *ibid.* **19**, 3649 (1986).
[31] J. H. Eberly, J. Javanainen, and K. Rzążewski, Phys. Rep. **204**, 331 (1991).
[32] M. Y. Ivanov and K. Rzążewski, J. Mod. Phys. **39**, 2377 (1992).
[33] N. B. Delone and V. P. Kraïnov, *Atoms in Strong Fields* (Springer-Verlag, Heidelberg, 1985); L. D. Landau, *Quantum Mechanics* (Pergamon, New York, 1964).
[34] R. Grobe and M. V. Fedorov, J. Phys. B **26**, 1181 (1993).
[35] J. J. Macklin, private communication.
[36] H. A. Bethe and E. E. Salpeter, *Quantum Mechanics of One and Two Electron Atoms* (Academic, New York, 1957).
[37] S. Geltman, Phys. Rev. A **45**, 5293 (1992).
[38] R. Grobe and M. V. Fedorov, Phys. Rev. Lett. **68**, 2595 (1992).
[39] M. Yu. Ivanov (unpublished).